Kinetic and Spectroscopic Studies of *Tritrichomonas foetus* Low-Molecular Weight Phosphotyrosyl Phosphatase. Hydrogen Bond Networks and Electrostatic Effects†

Christin L. Thomas,‡ Evangeline McKinnon,‡ Bruce L. Granger,§ Etti Harms,|| and Robert L. Van Etten*,‡

Department of Chemistry, Purdue University, West Lafayette, Indiana 47907-1393, Department of Biological Sciences, Purdue University, West Lafayette, Indiana 47907, and Department of Microbiology, Montana State University, Bozeman, Montana 59717

Received May 21, 2002; Revised Manuscript Received September 18, 2002

ABSTRACT: Virtually all of the eukaryotic low-molecular weight protein tyrosine phosphatases (LMW PTPases) studied to date contain a conserved, high-pK_a histidine residue that is hydrogen bonded to a conserved active site asparagine residue of the phosphate binding loop. However, in the putative enzyme encoded by the genome of the trichomonad parasite *Tritrichomonas foetus*, this otherwise highly conserved histidine is replaced with a glutamine residue. We have cloned the gene, expressed the enzyme, demonstrated its catalytic activity, and examined the structural and functional roles of the glutamine residue using site-directed mutagenesis, kinetic measurements, and NMR spectroscopy. Titration studies of the two native histidine residues in the *T. foetus* enzyme as monitored by ^{1}H NMR revealed that H44 has a pK_a of 6.4 and H143 has a pK_a of 5.3. When a histidine residue was introduced in place of the native glutamine at position 67, a pK_a of 8.2 was measured for this residue. Steady state kinetic methods were employed to study how mutation of the native glutamine to alanine, asparagine, and histidine affected the catalytic activity of the enzyme. Examination of k_{cat}/K_m showed that Q67H exhibits a substrate selectivity comparable to that of the wild-type (WT) enzyme, while Q67N and Q67A show reduced activity. The effect of pH on the reaction rate was examined. Importantly, the pH−rate profile of the WT TPTP enzyme revealed a much more clearly defined acidic limb than that which can be observed for other wild-type LMW PTPases. The pH−rate curve of the Q67H mutant shows a shift to a lower pH optimum relative to that seen for the wild-type enzyme. The Q67N and Q67A mutants showed curves that were shifted to higher pH optima. Although the active site of this enzyme is likely to be similar to that of other LMW PTPases, the hydrogen bonding and electrostatic changes afford new insight into factors affecting the pH dependence and catalysis by this family of enzymes.

Phosphorylation and dephosphorylation of tyrosine residues are important events in cell cycle function and regulation. Phosphatases and kinases play crucial roles in maintaining the balance between the phosphorylated and unphosphorylated states. Protein tyrosine phosphatases (PTPases)[1] are important in cell cycle regulation and intracellular signaling, including critical processes that have been implicated in cancer, insulin action, and cell growth and development (*1*−*3*). On the basis of size and substrate specificity, several subfamilies may be recognized that share little sequence similarity apart from the highly conserved active site sequence, CX_5R. One subfamily is composed of the high-molecular weight enzymes that occur as both membrane-bound receptors and cytosolic enzymes. They share a conserved catalytic domain of 250 amino acids and a similar α/β folding architecture. A second subfamily is composed of the dual-specificity PTPases that show catalytic activity toward phosphotyrosine as well as phosophoserine and phosphothreonine. These enzymes contain a catalytic domain of approximately 170 amino acids. The third subfamily is comprised of the low-molecular weight PTPases (LMW PTPases). With the exception of the structure of the phosphate binding loop (the P-loop), the LMW PTPases show no apparent structural similarity to the other PTPase families (*4*).

The LMW PTPases are cytosolic enzymes that are ubiquitous in eukaryotes and are characterized by their size (<18 kDa), the presence of the active site signature motif near the N-terminus, and a high degree of overall sequence similarity. Despite the low level of sequence and structural

† This work was supported by Department of Health and Human Services National Institutes of Health Grant GM 27003.

* To whom correspondence should be addressed. Fax: (765) 494-0239. E-mail: vanetten@purdue.edu.

‡ Department of Chemistry, Purdue University.

§ Montana State University.

|| Department of Biological Sciences, Purdue University.

[1] Abbreviations: PTPase, protein tyrosine phosphatase; LMW PTPase, low-molecular weight protein tyrosine phosphatase; HMW PTPase, high-molecular weight protein tyrosine phosphatase; BPTP, bovine protein tyrosine phosphatase; TPTP, *Tritrichomonas foetus* protein tyrosine phosphatase; DCl, deuterium chloride; NaOD, sodium deuterioxide; D_2O, deuterium oxide; CD, circular dichroism; DSS, 2,2-dimethyl-2-silapentane-5-sulfonate; DTT, dithiothreitol; WT, wild-type; EDTA, ethylenediaminetetraacetic acid disodium salt dihydrate; BSA, bovine serum albumin; IPTG, isopropyl β-D-thiogalactoside; LB, Lenox broth; MALDI-MS, matrix-assisted laser desorption ionization mass spectrometry; PCR, polymerase chain reaction; k_{cat}, catalytic rate constant or turnover number; K_m, Michaelis−Menten constant; NMR, nuclear magnetic resonance; *p*-NPP, *p*-nitrophenyl phosphate; SDS−PAGE, sodium dodecyl sulfate−polyacrylamide gel electrophoresis; V_{max}, enzyme velocity at a saturating substrate concentration.

10.1021/bi0203740 CCC: $22.00
Published on Web 12/03/2002

similarity between the subfamilies of PTPases, they exhibit similar catalytic mechanisms, and the LMW enzymes serve as useful models for the more complex PTPases. The enzymes are active over a wide pH range and act on several different synthetic phosphomonoesters in vitro. A number of putative substrates have been examined in vitro and in vivo, but the functions of these enzymes in the cell have not been established with certainty (cf. refs *5* and 6).

In the first step of the reaction catalyzed by LMW PTPases, the reaction is initiated by donation of a proton from a highly conserved aspartic acid residue to the oxygen of the leaving tyrosyl group of the bound phosphomonoester (*7*). As the reaction progresses, a covalent phosphoenzyme intermediate is formed by phosphoryl transfer from the phosphotyrosine substrate to a nucleophilic cysteine that is part of the active site signature motif (*8*−*10*). The second step of the mechanism involves a generally rate-limiting hydrolysis of the covalent phosphoenzyme intermediate which leads to formation of the final product, inorganic phosphate (*11*, 12). The transition states for these steps are highly dissociative in character, a conclusion that follows from not only comprehensive kinetic isotope measurements but also recent density functional calculations (*13*, *14*).

The similar catalytic mechanism among all PTPases is facilitated by a shared structural feature known as the phosphate binding loop, or P-loop. The P-loop is formed by the amino acids in the conserved active site sequence, CX_5R, and it serves to position the substrate for nucleophilic attack. In HMW PTPases, this motif contains several glycines which allows the P-loop to adopt a conformation well suited to binding phosphate. Among the eukaryotic LMW PTPases, the active site P-loop motif CXGNXCRS contains a single glycine (Figure 1). Despite this difference, structural comparison of P-loop positions in known PTPase structures shows this region is highly superimposable (*4*). This structural similarity depends in part on interactions with residues outside of the P-loop.

In addition to the P-loop residues, the LMW PTPases also contain other highly conserved residues, including E23, D42, S43, H72, D129, Y131, and Y132 (all numbering is based on the BPTP sequence). Studies have shown that many of these residues are important for the structure and function of the enzymes (*7*, *9*, 15−*18*). In particular, mutation of the highly conserved H72 in BPTP to asparagine or alanine resulted in enzymes with moderately or highly reduced activity, respectively (*15*, 19). Further studies demonstrated that the change in activity was not due to a change in the rate-determining step of the catalytic mechanism. Instead, crystallographic determinations revealed that in the P-loop, N15 is found in a strained, left-handed conformation which alters the P-loop backbone such that the NH groups of the active site loop are oriented toward the phosphate ion and the overall conformation resembles that of the glycine-rich P-loop of HMW PTPases (*4*, *16*). As shown in Figure 2, H72 is part of an extensive hydrogen bonding network involving elements of the active site, including a hydrogen bond to the side chain of N15 that is critical in stabilizing this residue in its otherwise energetically unstable conformation (*4*, *16*). H72 is also involved in a number of significant electrostatic interactions that are important for active site stabilization and orientation of the phosphorylated substrate (*16*, *17*). In BPTP, the reduced activity of the H72N mutant was attributed to structural changes within the active site due to reorganization of the hydrogen bonding network (*16*, *19*, 20).

Histidine residues are very sensitive to electrostatic effects of nearby amino acids and can act as reporter groups concerning the local environment. For example, titration of the two histidines in WT BPTP, H66 and H72, showed they have pK_a values of 8.4 and 9.2, respectively (*19*, *21*). These pK_a values are significantly elevated relative to a value of approximately 6.5 expected for an unperturbed histidine side chain. The pK_a perturbation of H72 was due primarily to the presence of two nearby anionic side chains, E23 and D42, but hydrogen bonding interactions also contribute (*16*, *18*, *20*, *21*).

In this paper, we report the expression and characterization of a LMW phosphatase from the bovine protozoan parasite *Tritrichomonas foetus*. These primitive eukaryotic organisms do not contain mitochondria or peroxisomes, but instead contain hydrogenosomes, which are double-membrane-bound organelles that are involved in metabolic processes that extend glycolysis (*22*, 23). The parasite resides in the urogenital tract of cattle and is responsible for asymptomatic infection in bulls, but inflammation, infertility, and abortion in cows. The organism is responsible for great economic loss in the agricultural industry, but the mechanism of virulence is largely unknown (*24*). Because a PTPase is fundamental to the virulence of *Yersinia pestis*, and a LMW PTPase has been identified as part of the virulence gene cluster of *Erwinia amylovora*, we are studying the *T. foetus* enzyme (TPTP) (*25*, 26).

The LMW PTPase encoded by the genome of *T. foetus* contains the characteristic, highly conserved active site sequence and the catalytically important aspartic acid residue (Figure 1). In addition, it encodes many other residues, analogous to E23, D42, and S43 in BPTP, which make up the active site and its hydrogen bonding network. It does not, however, contain the otherwise fully conserved histidine (H72 in BPTP) that has been demonstrated to be important for enzyme structure and activity. It is the only known eukaryotic LMW PTPase that does not possess this residue.[2] We sought to explore the activity of the TPTP enzyme and the possible structural and functional roles of the Q67 residue, which is in a position homologous to that of H72 in the bovine enzyme. A series of mutagenesis and kinetic experiments with recombinant TPTP enzymes have been carried out in an effort to examine the role of the unique glutamine residue. Because the structure of TPTP is not known, mutagenesis and histidine titration experiments were also carried out to probe electrostatic effects at the active site and to obtain basic structural information that would complement the kinetic studies.

EXPERIMENTAL PROCEDURES

Materials. IPTG, SP-Sephadex C-50 beads, and *p*-nitrophenyl phosphate disodium salt were from Sigma, Sephadex G-50 and G-75 beads from Pharmacia, and Omega 3K membranes from Filtron. Chemicals used in the modified

[2] The recently reported primo-2 putative low-molecular weight tyrosine phosphatase from *Drosophila* shows the conserved histidine interchanged with glycine in the usual alignment position. The glycine is presumably flexible and should allow this histidine to have the same structural role.

```
TPTP       S--AEKKAVLFVCLGNICRSPACEGICRDMVGDKLI------IDSAA       39
BPTP       AEQVTKS-VLFVCLGNICRSPIAEAVFRKLVTDQNISDNW-VIDSGA       45
HPTPB      AEQATKS-VLFVCLGNICRSPIAEAVFRKLVTDQNISENW-VIDSGA       45
HPTPA      AEQATKS-VLFVCLGNICRSPIAEAVFRKLVTDQNISENW-RVDSAA       45
RATACP1    AEVGSKS-VLFVCLGNICRSPIAEAVFRKLVTDENVSDNW-RIDSAA       45
RATACP2    AEVGSKS-VLFVCLGNICRSPIAEAVFRKLVTDENVSDNW-AIDSSA       45
DPRIMO1    VRK-----VLMICLGNICRSPIAEVVMVDTLEKANVKDV--EVDSAA       40
DPRIMO2    GKRSQKSSVLMVCVGNLCRSPIAEAVMRDVVARAGLQGEW-HVESAG       46
Ltp1       TIEKPKISVAFICLGNFCRSPMAEAIFKHEVEKANLENRFNKIDSFG       47
Stp1       T---KNIQVLFVCLGNICRSPMAEAVFRNEVEKAGLEARFDTIDSCG       44
                 ^^ ^  ^         ^  ^ ^^   ^       ^^  ^

TPTP       TSGFHVGQSPDTRSQKVCKSNGVDISKQRARQITKADFSKFDVIAAL       86
BPTP       VSDWNVGRSPDPRAVSCLRNHGINTA-HKARQVTKEDFVTFDYILCM       91
HPTPB      VSDWNVGRSPDPRAVSCLRNHGIHTA-HKARQITKEDFATFDYILCM       91
HPTPA      TSGYEIGNPPDYRGQSCMKRHGIPMS-HVARQITKEDFATFDYILCM       91
RATACP1    TSTYEVGNPPDYRGQNCMKKHGIHMQ-HIARQITREDFATFDYILCM       91
RATACP2    VSDWNVGRPPDPRAVNCLRNHGISTA-HKARQITREDFATFDYILCM       91
DPRIMO1    IGGWHVGNRADPRAISTLQKHGLKCT-HIVRQIRKQDFSEFDYIFGM       86
DPRIMO2    IEDWHSGHQPDERALNVLARHNIEYH-GKARVLAPEDFLEFDYIFAM       92
Ltp1       TSNYHVGESPDHRTVSICKQHGVKIN-HKGKQIKTKHFDEYDYIIGM       93
Stp1       TGAWHVGNRPDPRTLEVLKKNGIHTK-HLARKLSTSDFKNFDYIFAM       90
           ^^^^^    ^   ^ ^    ^^^       ^ ^   ^  ^^     ^

TPTP       DQSILSDINSMKPS--NCRAKVVLFNP--------PNGVDDPYYSS       122
BPTP       DESNLRDLNRKSNQVKNCRAKIELLGSYD-PQKQL--IIEDPYYG-       133
HPTPB      DESNLRDLNRKSNQVKTCKAKIELLGSYD-PQKQL--IIEDPYYG-       133
HPTPA      DESNLRDLNRKSNQVKTCKAKIELLGSYD-PQKQL--IIEDPYYG-       133
RATACP1    DESNLRDLNRKSNQVKNCKAKIELLGSYD-PQKQL--IIEDPYYG-       133
RATACP2    DESNLRDLNRKSNQVKNCKAKIELLGSYD-PQKQL--IIEDPYYG-       133
DPRIMO1    DEDNMSELRRLAP--KGSKAELLMLGDFGLEKKNR--IIEDPYYER       128
DPRIMO2    DLSNLAALRRMAP--KGTTVKLLILGNFGLKPDER--IIEDPYYDI       134
Ltp1       DESNINNLKKIQPE--GSKAKVCLFGDWNTNDGTVQTIIEDPWYG-       136
Stp1       DSSNLRNINRVKPQ--GSRAKVMLFGEYASPG--VSKIVDDPYYG-       131
             ^ ^ ^^^^      ^  ^^^ ^^^           ^^  ^ ^

TPTP       D--GFPTMFASISKEMKPFLTEHGL---I                        146
BPTP       NDADFETVYQQCVRCCRAFLEKVR-----                        157
HPTPB      NDSDFETVYQQCVRCCRAFLEKAH-----                        157
HPTPA      NDSDFETVYQQCVRCCRAFLEKAH-----                        157
RATACP1    NDSDFEVVYQQCLRCCKAFLEKTH-----                        157
RATACP2    NDSDFEVVYQQCLRCCKAFLEKTH-----                        157
DPRIMO1    GAEGFETAYQQCVVACAAFMKE---RLQK                        154
DPRIMO2    GEASFEEIYRQCSIACRNFLKQARLKQIM                        163
Ltp1       DIQDFEYNFKQITYFSKQFLKKE-----L                        160
Stp1       GSDGFGDCYIQLVDFSQNFLKSI-----A                        155
           ^  ^     ^           ^^
```

FIGURE 1: Alignment of representative eukaryotic low-molecular weight protein tyrosine phosphatases from *T. foetus* (TPTP), bovine (BPTP), human (HPTPA and HPTPB isoenzymes), rat (RATACP-1 and -2 isoenzymes), *Drosophila* primo locus (DPRIMO-1 and -2), *Saccharomyces cerevisiae* (Ltp1), and *Schizosaccharomyces pombe* (Stp1). Conserved residues are shown in bold, and a caret (∧) is used to show a conservative amino acid substitution. The highly conserved histidine found in the hydrogen bonding network is outlined in gray. The numbering does not include the initial methionine which is removed during processing to the mature enzyme.

Lowry and BCA assays were from Pierce. All other chemicals were from Sigma or Aldrich. Oligonucleotide primers were synthesized at Integrated DNA Technologies (IDT) Inc. (Coralville, IA). The DCl, DSS, and D_2O used in pH titration experiments were from Cambridge Isotope Laboratories. The NaOD was from Aldrich, and pH calibration standards were from Fisher Scientific.

Subcloning of the TPTP Gene. A putative PTPase was identified in a 2387 bp *Eco*RI−*Kpn*I fragment of genomic DNA from *T. foetus* strain MT85-330.1 cloned into pBluescript KS+ plasmid "pKE-2" (see GenBank accession number U66070). Transcription of this gene in *T. foetus* was confirmed by S1 nuclease protection analysis, which also identified the transcription start site as being 13−15 bases upstream from the start codon (TCAT*T*T*T*ACTTTTTTCTAAAAATG) (unpublished results and ref *27*). For production of useful amounts of the recombinant protein, the coding sequence was amplified from pKE-2 by polymerase chain reaction (*28*) and subcloned into expression vector pET23d (Novagen). The forward primer 5′-GTCTACCATGGCTGCAGAAAAGAAAGCTGTG-3′ contained an *Nco*I restriction site, whereas the reverse primer 5′-GAAATATAAGCTTAGATAAGGCCGTATTCAGTAAGG-3′ contained a *Hin*dIII site. The PCR product was purified, digested with *Nco*I and *Hin*dIII, and resolved by agarose gel electrophoresis. The 444 bp product was excised, purified, ligated into similarly cut pET23d, and transformed into *Escherichia coli* strain BL21(DE3).

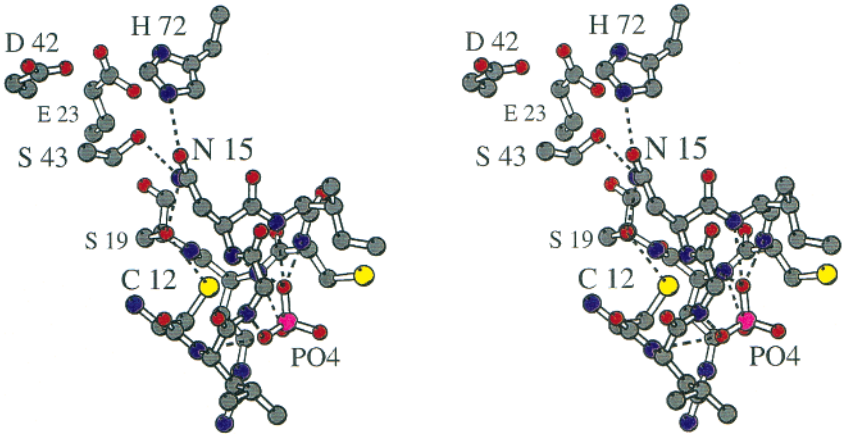

FIGURE 2: Stereoview of the active site of BPTP (PDB entry 1PNT), showing the residues that participate in the active site hydrogen bonding network involving C12, N15, S19, S43, and H72. Also shown are the NH interactions of residues of the phosphate binding loop with the bound phosphate ion. Also shown are residues E23 and D42 that are responsible for the elevated pK_a of H72 (*4*).

A pET23d plasmid containing the coding sequence for the PTPase gene of *T. foetus* was named pTritri; its sequence was confirmed using the method of Sanger (*29*). Mutagenesis was performed using synthetic oligodeoxynucleotide primers and a QuikChange site-directed mutagenesis kit from Stratagene. Primers were designed to create the following mutations in WT TPTP: A1S, H44A, H143A, Q67H, Q67N, and Q67A. Mutated plasmids were transformed into *E. coli* BL21-(DE3) cells and their sequences confirmed as described above.

Expression of Recombinant TPTP. *E. coli* BL21(DE3) cells harboring the WT and mutant pTritri plasmids were grown in 10 mL of LB medium containing 50 μg/mL ampicillin while shaking for 10−12 h at 37 °C. The culture was then diluted 1:20 into fresh LB medium containing 50 μg/mL ampicillin and incubated for an additional 10−12 h. Finally, this culture was diluted 1:10 into fresh LB medium containing 50 μg/mL ampicillin and was incubated until an OD_{600} measurement between 0.6 and 1 was achieved. IPTG was added to a final concentration of 0.4 mM, and the cells were incubated for an additional 3−4 h. The cells were harvested by centrifugation, washed with 0.85% NaCl, and either lysed immediately or stored at −20 °C for later use.

Prior to cell lysis, the bacterial pellet was resuspended in low-ionic strength buffer [10 mM NaOAc, 10 mM NaH_2PO_4, and 1 mM EDTA (pH 4.8)] containing 1 mM DTT. The suspension was then passed three times through a French press (SLM Instruments, model SLM AMINCO) at 15 000 psi. The lysed cell suspension was centrifuged, and the supernatant was loaded onto a SP-Sephadex C-50 cation-exchange column pre-equilibrated with low-ionic strength buffer and washed to remove unbound protein. The PTPase was eluted with a linear gradient of low-ionic strength buffer and elution buffer [300 mM NaH_2PO_4, 60 mM NaCl, and 1 mM EDTA (pH 5.1)]. Fractions with the highest specific activity were combined and concentrated using an Amicon 3K ultrafiltration apparatus. The concentrate was loaded onto a Sephadex G-50 or G-75 size-exclusion column that had been pre-equilibrated with buffer containing 10 mM NaOAc, 30 mM NaH_2PO_4, 60 mM NaCl, and 1 mM EDTA (pH 4.8). Fractions containing the purest enzyme, assessed by their specific activities and SDS−PAGE, were combined and concentrated as described above for further analyses. The N-terminal amino acid sequence of the expressed protein was confirmed by direct sequencing (data not shown).

Enzyme Concentration and Specific Activity Measurement. Phosphatase activity was measured in activity assay buffer [100 mM sodium acetate and 1 mM EDTA (pH 5.0) with an ionic strength of 150 mM adjusted with NaCl] containing 2−10 mM *p*-NPP, the mixture incubated at 37 °C for 4 min, and the reaction quenched with 1 M NaOH. *p*-Nitrophenolate product was assessed at 405 nm. Protein concentrations were initially estimated using the absorbance at 280 nm and a molar extinction coefficient of 2560 M^{-1} cm^{-1} (estimated using PCGene; note that this enzyme contains no tryptophan). Subsequent determinations employed a modified Lowry assay or BCA assay.

Circular Dichroism. The CD spectra of wild-type and mutant TPTP proteins were recorded on a JASCO model J810 spectropolarimeter over the range of 190−260 nm using a 0.5 cm cell. Protein concentrations were 4.7 μM in 10 mM sodium phosphate buffer (pH 5.0).

Substrate Specificity and Reversible Inhibition. Except for the case of the *p*-NPP substrate, enzyme activity was quantitated by the measurement of inorganic phosphate release with molybdate and ascorbic acid in the presence of arsenate (*30*). The potential substrate, at concentrations ranging from 0.1K_m to 10K_m, was incubated with assay buffer at 37 °C, and the reaction was initiated by the addition of a catalytic amount of enzyme. After the reaction was allowed to proceed for 4−8 min (established in each case to be within the linear initial velocity range), it was quenched by the addition of 10% trichloroacetic acid. The color was developed 15−30 min after the addition of the molybdate and ascorbic acid, and the absorbance at 700 nm was measured. The amount of inorganic phosphate produced was calculated from a standard curve obtained using KH_2PO_4.

Inhibition studies were all conducted in the pH 5.0 assay buffer at *p*-NPP substrate concentrations from 0.1K_m to 10K_m. The initial velocities were measured at 8−10 different inhibitor concentrations. After the mixture had been incubated for 10 min at 37 °C, the reaction was quenched by the addition of 1 M NaOH. The absorbance at 405 nm was measured and used with the extinction coefficient of *p*-NPP (18 000 M^{-1} cm^{-1} for *p*-nitrophenolate) to calculate the specific activity of the enzyme against *p*-NPP. The kinetic parameters k_{cat} and K_m were calculated by a nonlinear least-squares fit of the Michaelis−Menten equation to the observed data using SigmaPlot (Jandel Scientific). The inhibition

constants were calculated from Dixon plots of the reciprocal initial velocity versus inhibitor concentration.

Steady State Kinetics. The phosphatase activities of the purified enzymes were measured with the synthetic substrate *p*-NPP at pH 5.0 and 37 °C. Reactions were initiated by adding a sufficiently concentrated amount of enzyme to a mixture of assay buffer and *p*-NPP substrate. The enzyme stock solution and assay buffer/substrate mixture all contained 0.1 mg/mL BSA to reduce the extent of nonspecific binding of enzyme to glass and plastic during activity measurements. At least 12 substrate concentrations were used between $0.1K_m$ and $10K_m$ for the WT and mutant enzymes. Assay linearity over at least 10 min was established, but for convenience, only 4 min points were used. All assays were done in triplicate at 37 °C. Samples were processed and analyzed as described above.

pH−Rate Profile. A series of assay buffers containing 1 mM EDTA and adjusted to an ionic strength of 150 mM with NaCl were used in the pH dependence studies. The assay buffers were 100 mM sodium acetate (pH 4.0−5.5), 100 mM Bis-Tris (pH 6.0−6.5), and 100 mM Tris (pH 7.0). At least six different concentrations of substrate (*p*-NPP) were used, ranging from approximately $0.1K_m$ to $10K_m$ at each pH. Reactions and calculations were conducted by the method given above. The pH data were fit to eq 1 using nonlinear least-squares analysis with Igor Pro (Wavemetrics Inc.).

$$k_{cat}/K_m = \frac{(k_{cat}/K_m)_c}{(1 + H/K_s)(1 + H/K_1 + K_2/H)} \quad (1)$$

where $(k_{cat}/K_m)_c$ is the pH-independent value of the pseudo-second-order rate constant, H is the hydrogen ion concentration, K_s is the second ionization constant of the substrate, and K_1 and K_2 are ionization constants of the free enzyme.

Nuclear Magnetic Resonance Spectroscopy. Protein samples were prepared for spectroscopy according to the method of Tishmack *et al.* (*21*). Proton NMR spectroscopy was carried out at 25 ± 1 °C on a Varian Unity Plus 600 MHz spectrometer. The spectral widths were between 7200 and 7585 Hz. For 1-1 echo spectra, 128 scans were acquired with the echo delay time set to 40 ms with an acquisition time of 1 s. Spectra were processed with 32K points, a 0.2 s Gaussian function, and baseline correction. The spectra were referenced to an internal DSS standard, and the intense H_2O signal was further reduced with the Varian solvent suppression algorithm.

pH Titrations and pK_a Calculations. The pH titrations were performed according to the method of Tishmack *et al.* (*21*). Calculations of histidine pK_a values were carried out using a modified Hill equation together with a Marquardt−Levenberg nonlinear least-squares fitting algorithm (eq 2) (SigmaPlot, Jandel Scientific) (*31*, 32).

$$\delta_{ob} = \delta_A + (\delta_{AH} - \delta_A)(10^{-pK_a/n})/(10^{-pK_a/n} + 10^{-pH/n}) \quad (2)$$

where δ_A is the chemical shift of the unprotonated species, δ_{AH} is the chemical shift of the protonated species, and n is the Hill coefficient.

RESULTS

Cloning. For convenience in constructing an expression system for the putative PTPase gene from *T. foetus*, the first codon following the start codon was mutated from TCA to GCT to provide an additional restriction site. Thus, the expressed enzyme began with an AlaAla motif instead of a SerAla motif. Crystal structures of the bovine, human, and yeast enzymes all show that the first four N-terminal residues are highly disordered (*16*, *33*, *34*). On the basis of these observations, it was anticipated that an N-terminal mutation in TPTP would not have a measurable effect on the protein structure or activity. This was confirmed by direct activity measurements with both the AlaAla and SerAla purified proteins. Accordingly, results obtained using this N-terminal AlaAla protein are also denoted as being obtained with the wild-type (WT) protein.

Table 1: Kinetic Parameters of WT and Mutant TPTP Using *p*-NPP as the Substrate[a]

enzyme	K_m (mM)	V_{max} (units/mg)	k_{cat} (s^{-1})	k_{cat}/K_m ($\times 10^{-3}$ M^{-1} s^{-1})
WT	0.20 ± 0.02	32.7 ± 0.6	8.6 ± 0.1	44 ± 4
A1S	0.20 ± 0.01	27.5 ± 2.2	7.3 ± 0.6	36 ± 3
H44A	0.17 ± 0.01	32.3 ± 1.9	8.5 ± 0.5	51 ± 1
H143A	0.19 ± 0.01	29.8 ± 4.3	7.8 ± 1.1	42 ± 5
Q67A	0.51 ± 0.01	24.9 ± 0.2	6.5 ± 0.1	13 ± 0.4
Q67H	0.46 ± 0.12	72.5 ± 4.1	19.1 ± 1.1	44 ± 9
Q67N	0.35 ± 0.07	30.7 ± 1.8	8.1 ± 0.5	24 ± 6

[a] Measurements were taken at pH 5.0 and 37 °C in 100 mM sodium acetate, 1 mM EDTA, and NaCl to give an ionic strength of 150 mM.

Overexpression and Purification of WT TPTP and Mutants. A T7 RNA polymerase-dependent expression system was used to overexpress WT and mutant enzymes in *E. coli* BL21(DE3) cells (*35*). The following mutants were constructed from the WT clone: H44A, H143A, Q67N, Q67H, Q67A, and A1S. Large-scale expression of the WT and mutant enzymes produced milligram quantities of the purified protein. Two chromatographic steps, a cation-exchange column followed by a size-exclusion column, were sufficient to purify the proteins to homogeneity. MALDI-MS was used to confirm the size and purity of the expressed proteins (data not shown).

Circular Dichroism Analysis. Circular dichroism was used to confirm the structural integrity of the WT TPTP and mutants (data not shown). Comparison of the spectra indicated that the overall secondary structure was retained and that the mutations had not caused misfolding of the proteins. This is also consistent with ^{1}H NMR data (vide infra).

Steady State Kinetics and Substrate Specificity. Michaelis−Menten kinetic parameters were determined for WT and mutant enzymes with *p*-NPP as the substrate (Table 1). Kinetic properties of the A1S mutant confirmed that the S1A mutation (introduced during cloning) did not significantly affect enzyme activity. The substrate specificity of the WT LMW PTPase cloned from *T. foetus* was relatively similar to those of other LMW PTPases (*36*−*39*) (Table 2). The following competitive inhibition constants were measured: 7.6 mM for inorganic phosphate, 95 μM for vanadate, 90 μM for pyridoxal phosphate, and >26 mM for HEPES.

Both of the native histidines of WT TPTP (H44 and H143) were mutated to alanine in an effort to assign the ^{1}H NMR histidine proton resonances. The H44A and H143A enzymes retained near-WT activity, and no significant changes in K_m were observed.

Point mutations were made at position 67 to explore the role of the glutamine, including its possible participation in

Table 2: Substrate Specificities of the *T. foetus* LMW PTPase[a]

substrate	K_m (mM)	k_{cat} (s^{-1})	k_{cat}/K_m ($\times 10^{-3}$ M^{-1} s^{-1})
p-nitrophenyl phosphate	0.21	8.0	38
phosphotyrosine	10.8	2.7	0.25
phosphoserine	ND[b]		
phosphothreonine	ND[b]		
β-naphthyl phosphate	8.7	5.7	0.65
α-naphthyl phosphate	ND[b]		
phenyl phosphate	8.6	5.7	0.66

[a] Measurements were taken at pH 5.0 and 37 °C in 100 mM sodium acetate, 1 mM EDTA, and NaCl to give an ionic strength of 150 mM. [b] Not measurable (the specific activity with 10 mM substrate was less than 2% of that with 10 mM *p*-NPP).

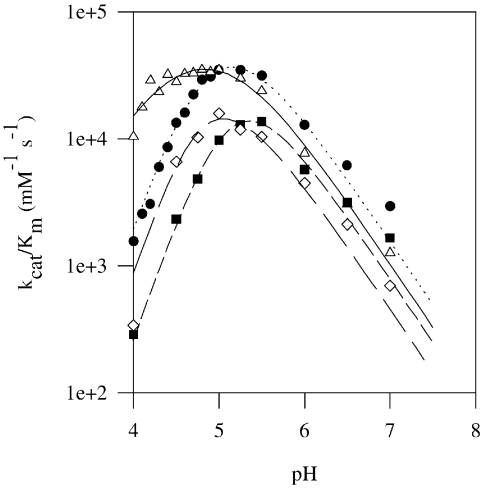

FIGURE 3: k_{cat}/K_m pH−rate profiles of WT TPTP and mutant enzymes: WT (●), Q67H (△), Q67N (◇), and Q67A (■). All data were fit to eq 1 as described in Experimental Procedures.

a hydrogen bonding network. The residue was mutated to asparagine, alanine, and histidine. The Q67A, Q67N, and Q67H enzymes had 2.5-, 1.8-, and 2.3-fold increases in K_m, respectively (Table 1). The Q67N mutant of TPTP showed an almost complete retention of wild-type enzymatic activity, while the Q67A mutant showed a k_{cat} which was 67% of that of the WT enzyme. Interestingly, the k_{cat} value observed for the Q67H enzyme was 2-fold greater than that of WT TPTP.

Substrate Selectivity Constants k_{cat}/K_m. The observed k_{cat}/K_m value for Q67H TPTP was effectively identical to that of the WT enzyme (Table 1). In contrast, the Q67A and Q67N mutants exhibited 3.4- and 1.8-fold decreases in k_{cat}/K_m, respectively, compared to that of WT TPTP. These values are consistent with an anticipated hydrogen bonding structural role of Q67 in the active site of the protein, and are similar to changes recently observed upon mutation of residues involved in the extended network of hydrogen bonds at the active sites of ketosteroid isomerase and manganese superoxide dismutase (*40*, *41*).

pH−Rate Profile. The effect of pH on activity was examined for WT, Q67H, Q67N, and Q67A TPTP in the pH range of 4.0−7.0. Plots of the pseudo-second-order rate constant k_{cat}/K_m as a function of pH reflect catalytically essential ionizations of the free enzyme and substrate. The curves shown in Figure 3 for TPTP and its mutants display an ascending slope of approximately 2 and a descending slope of approximately −1. Each curve was fit to eq 1 with one pK value fixed at 5.1, corresponding to the known second ionization constant of the *p*-NPP substrate (*42*). The estimated pK_a values for the free enzyme are given in Table 3. The slope of 2 is indicative of two unprotonated groups participating in the reaction. These are presumably the second ionization of the *p*-NPP substrate and ionization of the active site cysteine. The descending slope corresponds to the ionization of the essential aspartic acid residue (*7*). These assignments are consistent with both calculations and with experimental data for LMW PTPases and dual-specificity PTPases (*14*, *43*−*46*). It is clear that the active site nucleophile has an ionization constant that is much lower in magnitude than that of a typical thiol. This result is consistent with recent computational comparisons of PTPases (*43*). The limited range (at acidic pH) and the steepness of the leading edge of the profile for the Q67N and Q67A enzymes contribute to the difficulty of assigning values and to the large errors that are associated with the estimated values (*47*). In contrast, the Q67H curve is significantly shifted and gives a calculated cysteine pK_a of <4. The pK_a of the histidine was directly measured using NMR spectroscopy, and it is clearly not the titrating group that is measured here, since its pK_a is much higher (see the next section). The asparagine mutant showed a slight basic shift in the calculated pK_a values, although with a substantial error. The Q67A mutant showed a significant basic shift in the measured pK_a values.

Table 3: Calculated pK_a Values from the pH−Rate Profiles of k_{cat}/K_m[a]

enzyme	pK_{a1}	pK_{a2}	enzyme	pK_{a1}	pK_{a2}
WT	5.1 ± 0.2	4.7 ± 0.2	Q67N[b]	5.5 ± 1.5	4.1 ± 1.4
Q67H	<4	4.5 ± 0.2	Q67A	5.7 ± 0. 6	4.7 ± 0.5

[a] Measurements and calculations were completed according to the conditions given in Experimental Procedures. A value of 5.10 was assumed for the second ionization of free *p*-NPP. [b] The point at pH 4.0 was not included in the fit due to acid denaturation of the protein.

The pH−rate profiles of k_{cat} for the WT, Q67H, Q67N, and Q67A enzymes were effectively flat lines and virtually identical (data not shown). The profiles of k_{cat} versus pH reflect ionizations involved in the rate-limiting step of the mechanism after substrate binding up to release of products. In the case of the LMW PTPases, this would be the typically rate-limiting dephosphorylation of the phosphoenzyme intermediate (*11*). The lack of any pH dependence of k_{cat} in the pH range of 4−7 for this enzyme is in agreement with that observed for other members of the LMW PTPase subfamily (*48*, *49*). This is a distinct feature of the LMW PTPases.

^{1}H NMR and pH Titrations. Titrations of WT and Q67H TPTP were conducted to obtain information about the electrostatic environments of the histidine residues. Figure 4 shows ^{1}H NMR spectra of WT, H44A, H143A, and Q67H TPTP at pH 5.2 and 25 °C detected using a 1-1 echo pulse sequence.[3] This pulse sequence generally allows observation of the histidine C_2 and C_5 imidazole ^{1}H resonances in the region of 8−9 ppm by acting as a filtering method based on the differential transverse (T_2) relaxation time of protons (*50*, 51). The imidazole C_2 protons of histidine are spectroscopi-

[3] The peak seen at approximately 7.7 ppm in the spectrum labeled D is not a histidine resonance and did not shift as the sample was titrated.

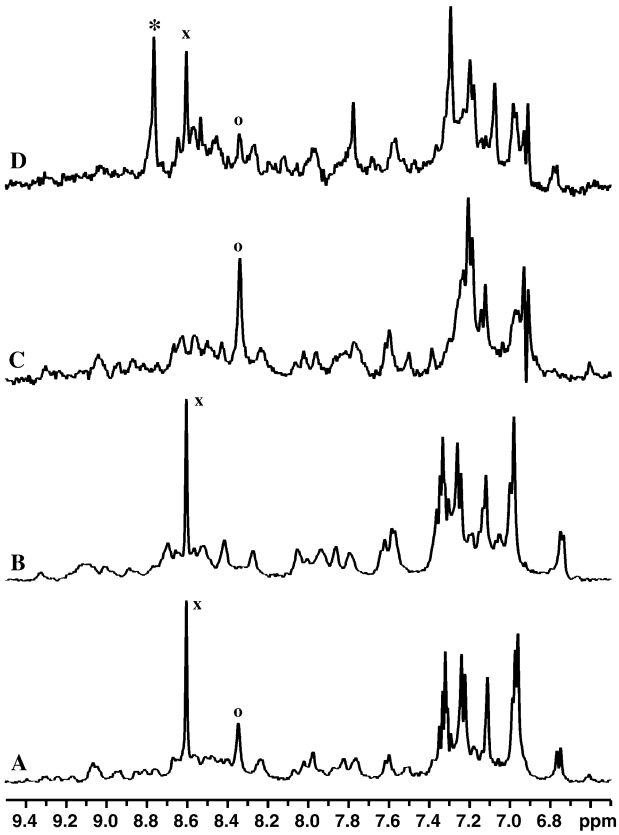

FIGURE 4: Selected 1-1 echo ^{1}H NMR spectra of TPTP and mutant proteins: (A) WT, (B) H44A, (C) H143A, and (D) Q67H. The H44 C_2H resonance is denoted with an x, the H143 C_2H resonance with an o, and the H67 C_2H resonance with an asterisk.[3] The protein concentration was 1−2 mM at pH 5.2 and 25 °C.

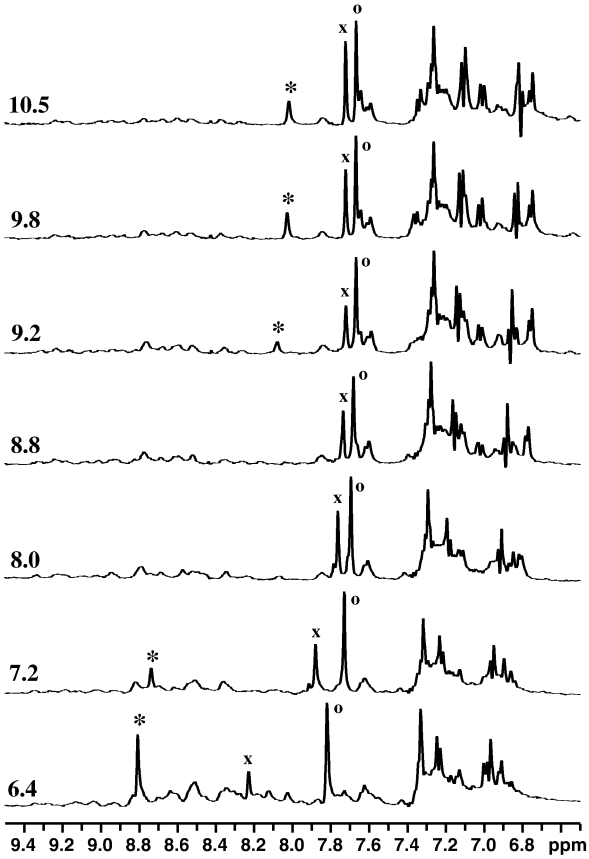

FIGURE 5: Selected 1-1 echo spectra of Q67H TPTP from pH 6.4 to 10.5 with conditions as described in Experimental Procedures. The pH is shown above the corresponding spectrum. The H44 C_2H resonance is denoted with an x, the H143 C_2H resonance with an o, and the H67 C_2H resonance with an asterisk. At pH 8.0 and 8.8, the H67 peak was too broad to be observed.

cally unique because they are found at a much higher frequency than most protons attached to carbon, and generally have narrower line widths (longer T_2 values) than other amide protons. These properties allow them to be distinguished and exploited in pH titration experiments. Peaks corresponding to histidine C_2 protons were identified and assigned by the absence of the corresponding peak in spectra of the specific alanine mutants. In the Q67H spectrum, the C_2 proton of H44 was identified as the peak at approximately 8.6 ppm, the C_2 proton of H143 was identified as the peak at approximately 8.35 ppm, and the C_2 proton of H67 was identified as the peak at approximately 8.8 ppm. The difference in the resolution and size of the H143 peak in the Q67H spectrum can be attributed to small differences in the pH and concentration among the samples. Histidine C_5 protons generally appear in the region of 5−7 ppm. However, in the spectra taken of the TPTP enzymes, they were difficult to distinguish and identify, and were therefore not utilized.

Figure 5 shows selected spectra from the pH titration experiment of Q67H TPTP over the pH range of 6.4−10.5, showing the complete titration of H67. (The H44 and H143 C_2 resonances can also be seen, but their titration is already substantially complete before pH 7.) During titration, the C_2 proton resonance of each histidine residue shifted to a lower frequency as the pH was increased. The aliphatic region (0−4 ppm) remained unchanged, indicating that the protein structure was not significantly altered by the pH changes (data not shown). As observed earlier for BPTP, broadening of the C_2 proton resonances in TPTP is observed in the

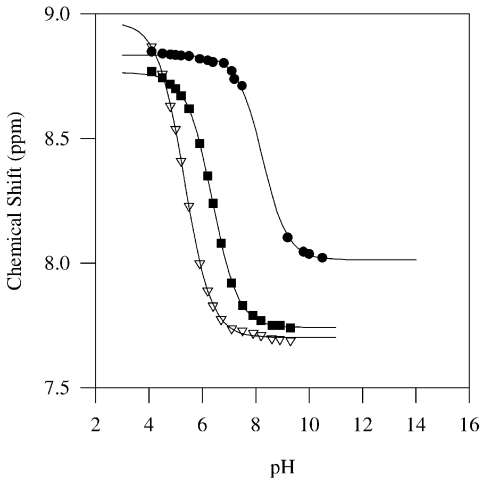

FIGURE 6: pH titration curves of TPTP H44 (■), H143 (▽), and H67 (●) imidazole side chains based on C_2H ^{1}H NMR chemical shifts. The solid lines are nonlinear least-squares fits of the data to the modified Hill equation (*21*, *32*).

transition region near the pK_a (*19*, *21*). The complete disappearance of the peaks is an artifact of the 1-1 echo filtering sequence that removes broad resonances.

A plot of the titration curves showing the chemical shift of the histidine imidazole C_2 protons as a function of pH for each histidine residue is shown in Figure 6. The data were fit to eq 2, and the calculated pK_a values can be seen in Table 4. Hill coefficients of near unity were found for

Table 4: Measured Histidine pK_a Values from ^{1}H NMR pH Titrations[a]

enzyme	residue	pK_a	enzyme	residue	pK_a
WT TPTP	H44	6.35 ± 0.02	Q67H TPTP	H67	8.19 ± 0.02
WT TPTP	H143	5.36 ± 0.003	Q67H TPTP	H143	5.36 ± 0.01
Q67H TPTP	H44	6.37 ± 0.01	WT BPTP	H72	9.19 ± 0.01

[a] Measurements were taken at 25 °C in 100 mM NaCl, 20 mM NaH_2PO_4, and 1 mM DSS on a Varian Unity$^+$ 600 MHz spectrometer. The BPTP value is from Tishmack *et al.* (*21*).

each titration curve, consistent with the conclusion that only one dissociating group was being titrated (*31*, *32*, 52).

DISCUSSION

As hypothesized on the basis of DNA sequence comparisons, the gene cloned from the trichomonad parasite *T. foteus* was demonstrated to encode a LMW PTPase enzyme. The expressed protein showed catalytic activity and substrate specificity toward phosphotyrosine and phosphotyrosine analogues similar to those of other LMW PTPases (*36*−*39*). The enzyme was also inhibited by inorganic phosphate, vanadate, and HEPES. Although pyridoxal phosphate appeared to act as a competitive inhibitor ($K_i = 90\ \mu$M), it is likely to be a substrate but with a sharply reduced k_{cat} (*53*).

An extensive hydrogen bonding network exists in the active site of LMW PTPases that is important for stabilizing the phosphate binding loop geometry needed for the optimal orientation and binding of the phosphorylated substrate and (particularly) the transition state (*16*, *17*, 54). The histidine residue that participates in the network is highly conserved among other eukaryotic species and is directly hydrogen bonded to a conserved asparagine in the PTPase P-loop motif (*16*, *17*). This asparagine is found in a strained, left-handed α-helical conformation that would be energetically unfavorable but appears to be stabilized by the interactions with H72, S19, and S43. The importance of the histidine in the hydrogen bonding network has also been demonstrated in enzyme stability measurements: the H72A mutant of the bovine enzyme showed a marked decrease in enzyme stability when compared to the WT enzyme (*17*). However, the enzyme isolated from the parasite *T. foetus* does not contain this otherwise highly conserved histidine residue. The corresponding residue appeared to be a glutamine, which presumably occupied the same position in the hydrogen bonding network as the highly conserved histidine. Unfortunately, the detailed structure of the enzyme is unknown, and numerous attempts to crystallize the protein have been unsuccessful. Therefore, a series of mutants were constructed to probe the structure and activity of this enzyme.

The native glutamine was mutated to histidine, asparagine, and alanine. As judged by circular dichroism, the resultant proteins showed apparently complete retention of secondary structure. For each of these enzymes, K_m was increased approximately 2-fold with respect to that of the WT enzyme. Although a reduced affinity for substrate may contribute to the overall observed increase in K_m, an unequivocal interpretation is difficult in the absence of pre-steady state kinetic measurements because it is known for the LMW enzymes that substrate K_m values are generally not true equilibrium binding constants (*12*).

When a histidine mutation was introduced to mimic the active sites of the other enzymes which contain the highly conserved histidine residue, the observed k_{cat} value for the Q67H enzyme was 2-fold *greater* than that of WT TPTP. Those LMW enzymes, in which a histidine residue is native, show somewhat higher specific activities toward *p*-NPP than does the WT TPTP enzyme (*8*, *36*, *37*, *39*, *55*). Despite the increased k_{cat} value, the k_{cat}/K_m value of the Q67H TPTP enzyme is identical to that of the WT enzyme.

The pH dependence of k_{cat}/K_m was explored for the WT, Q67H, Q67N, and Q67A mutants. Importantly, the WT curve exhibited an acidic limb that is more well-defined than any that can be experimentally observed with other LMW PTPases due to the onset of acid denaturation for those enzymes. This is a significant finding because the pK_a of the nucleophilic cysteine of those enzymes has been a matter of some controversy (*43*). The replacement of the native glutamine with histidine resulted in an acidic shift of the active site cysteine pK_a to <4 (Table 3), and the curve also more closely resembled that measured for the WT bovine enzyme (*17*). This value is lower than that measured for the other TPTP enzymes, but it is consistent with estimates made for the WT bovine enzyme (*17*). In WT BPTP, which possesses a histidine adjacent to the active site, the ionization constant of the nucleophilic cysteine could not be accurately determined due to acid-induced protein denaturation, but it was clearly below 4.0 (*17*). Consistent with earlier computational results, it is concluded that the presence of the histidine imidazolium ion side chain in the TPTP mutant and in the other WT enzymes helps to further stabilize the thiolate anion of the nucleophilic cysteine beyond that already caused by hydrogen bonding and dipolar interactions (*43*). The glutamine to alanine mutation resulted in an upward shift in the measured pK_a value (Table 3). Thus, the presence of the glutamine residue in TPTP, like histidine, helps to stabilize the active site in such a way that the nucleophilic cysteine is maintained in the anionic form at cellular pH.

The pK_a values of the histidines in the native protein and in the mutants of Q67 provided probes of their environment in the enzyme structure (*21*). The native residues, H44 and H143, do not exhibit unusual pK_a values. This is expected if the structure of TPTP is generally similar to the known structure of the bovine enzyme (*16*, *20*, *56*). On the basis of the BPTP structure, N50, the residue homologous to H44, is located on an exposed loop connecting β2 and α2. The residue corresponding to H143 of TPTP is V157, and it is located on the flexible C-terminus of BPTP (*16*, *20*). Consistent with this, the corresponding alanine mutants also show near-WT activity, indicating that the residues are not critical for structure or catalytic activity. The histidine residue introduced in TPTP by mutation of residue 67 has a measured pK_a value of 8.2. This may be compared with the elevated pK_a of 9.2 found for H72 of WT BPTP (*19*, *21*). In the BPTP enzyme, the pK_a of H72 is shifted upward by the presence of E23 and D42 (Figure 2) (*21*). Analogous residues, D36 and E22, are found in the TPTP primary sequence. Although the structure of the TPTP protein is unknown, it is reasonable to assume that the conformations of these residues place them in the proximity of the histidine that was introduced into position 67.

Potential Roles of Glutamine 67. HMW PTPases, protein kinases, and dehydrogenases have a glycine-rich P-loop, while the LMW PTPases only possess one glycine in their highly conserved CXGNXCRS P-loop motif. The high

superimposability of the P-loop structure from HMW and LMW PTPases despite the differences in P-loop composition demonstrates the importance of providing a specific conformation that allows optimal phosphate and transition state binding and stabilization. In LMW PTPases, this conformation is adopted in part because an asparagine residue (N15 in Figure 2) adopts an otherwise energetically unfavorable conformation by participating in an extensive hydrogen bonding network involving H72. These kinetic and spectroscopic studies indicate that the role of Q67 in the hydrogen bonding network is similar to that of H72 in BPTP and all other currently identified eukaryotic LMW PTPases. The altered kinetic constants of the TPTP enzyme upon mutation of this residue to histidine, asparagine, and alanine support this conclusion. This role is further supported by the relatively high pK_a of the non-native H67 residue. The electrostatic environment of the glutamine residue is apparently similar to that of the conserved histidine residues of other LMW PTPases. The glutamine residue is predicted to hydrogen bond with N14 of the P-loop, and thus indirectly contributes to substrate recognition and binding within the active site. The participation of this residue in the hydrogen bonding network also presumably imparts the enhanced thermodynamic stability as seen in the bovine enzyme (*17*). These results are consistent with the idea that the hydrogen bonding network is an integral contributor in maintaining the structure and activity of the low-molecular weight tyrosine phosphatases.

ACKNOWLEDGMENT

We thank Jennifer Laurence for her assistance with mutagenesis, Larry Riggs for kindly operating the MALDI-MS instrument, and Patrick Tishmack for his assistance with NMR spectroscopy and helpful comments on the manuscript.

REFERENCES

1. Li, L., and Dixon, J. E. (2000) *Semin. Immunol. 12*, 75−84.
2. Zhang, Z.-Y. (1998) *Crit. Rev. Biochem. Mol. 33*, 1−52.
3. Ramponi, G., and Stefani, M. (1997) *Biochim. Biophys. Acta 1341*, 137−156.
4. Zhang, M., Stauffacher, C. V., and Van Etten, R. L. (1995) *Adv. Protein Phosphatases 9*, 1−23.
5. Huang, L., Sankar, S., Lin, C., Kontos, C. D., Schroff, A. D., Cha, E. H., Feng, S. M., Li, S. F., Yu, Z., Van Etten, R. L., Blanar, M. A., and Peters, K. G. (1999) *J. Biol. Chem. 274*, 38183−38188.
6. Taddei, M. L., Chiarugi, P., Cirri, P., Talini, D., Camici, G., Manao, G., Raugei, G., and Ramponi, G. (2000) *Biochem. Biophys. Res. Commun. 270*, 564−569.
7. Zhang, Z., Harms, E., and Van Etten, R. L. (1994) *J. Biol. Chem. 269*, 25947−25950.
8. Wo, Y.-Y., Zhou, M.-M., Stevis, P., Davis, J. P., Zhang, Z.-Y., and Van Etten, R. L. (1992) *Biochemistry 31*, 1712−1721.
9. Cirri, P., Chiarugi, P., Camici, G., Manao, G., Raugei, G., Cappugi, G., and Ramponi, G. (1993) *Eur. J. Biochem. 214*, 647−657.
10. Davis, J. P., Zhou, M.-M., and Van Etten, R. L. (1994) *J. Biol. Chem. 269*, 8734−8740.
11. Zhang, Z.-Y., and Van Etten, R. L. (1991) *Biochemistry 30*, 8954−8959.
12. Zhang, Z.-Y., and VanEtten, R. L. (1991) *J. Biol. Chem. 266*, 1516−1525.
13. Hengge, A. C. (2002) *Acc. Chem. Res. 35*, 105−112.
14. Asthagiri, D., Dillet, V., Liu, T., Noodleman, L., Van Etten, R. L., and Bashford, D. (2002) *J. Am. Chem. Soc. 124*, 10225−10235.
15. Chiarugi, P., Cirri, P., Camici, G., Manao, G., Fiaschi, T., Raugei, G., Cappugi, G., and Ramponi, G. (1994) *Biochem. J. 298*, 427−433.
16. Zhang, M., Van Etten, R. L., and Stauffacher, C. V. (1994) *Biochemistry 33*, 11097−11105.
17. Evans, B., Tishmack, P. A., Pokalsky, C., Zhang, M., and Van Etten, R. L. (1996) *Biochemistry 35*, 13609−13617.
18. Tabernero, L., Evans, B. N., Tishmack, P. A., Van Etten, R. L., and Stauffacher, C. V. (1999) *Biochemistry 38*, 11651−11658.
19. Davis, J. P., Zhou, M.-M., and Van Etten, R. L. (1994) *Biochemistry 33*, 1278−1286.
20. Logan, T. M., Zhou, M.-M., Nettesheim, D. G., Meadows, R. P., Van Etten, R. L., and Fesik, S. W. (1994) *Biochemistry 33*, 11087−11096.
21. Tishmack, P. A., Bashford, D., Harms, E., and Van Etten, R. L. (1997) *Biochemistry 36*, 11984−11994.
22. Lindmark, D. G., and Muller, M. (1973) *J. Biol. Chem. 248*, 7724−7728.
23. Muller, M. (1993) *J. Gen. Microbiol. 139*, 2879−2889.
24. Speer, C. A., and White, M. W. (1991) *Large Anim. Vet. 46*, 18−20.
25. Guan, K. L., and Dixon, J. E. (1990) *Science 249*, 553−556.
26. Bugert, P., and Geider, K. (1997) *FEBS Lett. 400*, 252−256.
27. Granger, B. L., Warwood, S. J., Hayai, N., Hayashi, H., and Owhashi, M. (1997) *Mol. Biochem. Parasitol. 89*, 85−95.
28. Kleppe, K., Ohtsuka, E., Kleppe, R., Molineux, I., and Khorana, H. G. (1971) *J. Mol. Biol. 56*, 341−361.
29. Sanger, F., Nicklen, S., and Coulson, A. R. (1977) *Proc. Natl. Acad. Sci. U.S.A. 74*, 5463−5467.
30. Black, M. J., and Jones, M. E. (1983) *Anal. Biochem. 135*, 233−238.
31. Markley, J. L. (1975) *Acc. Chem. Res. 8*, 70−80.
32. Markley, J. L., and Finkenstadt, W. R. (1975) *Biochemistry 14*, 3562−3566.
33. Wang, S., Tabernero, L., Zhang, M., Harms, E., Van Etten, R. L., and Stauffacher, C. V. (2000) *Biochemistry 39*, 1903−1914.
34. Zhang, M., Stauffacher, C. V., Lin, D., and Van Etten, R. L. (1998) *J. Biol. Chem. 273*, 21714−21720.
35. Studier, F. W., Rosenberg, A. H., Dunn, J. J., and Dubendorff, J. W. (1990) *Methods Enzymol. 185*, 60−89.
36. Waheed, A., Laidler, P. M., Wo, Y.-Y., and Van Etten, R. L. (1988) *Biochemistry 27*, 4265−4273.
37. Zhang, Z.-Y., and Van Etten, R. L. (1990) *Arch. Biochem. Biophys. 282*, 39−49.
38. Ostanin, K., Pokalsky, C., Wang, S., and Van Etten, R. L. (1995) *J. Biol. Chem. 270*, 18491−18499.
39. Zhang, Z.-Y., Zhou, G., Denu, J. M., Wu, L., Tang, X., Mondesert, O., Russell, P., Butch, E., and Guan, K. L. (1995) *Biochemistry 34*, 10560−10568.
40. Kim, D. H., Jang, D. S., Nam, G. H., Choi, G., Kim, J. S., Ha, N. C., Kim, M. S., Oh, B. H., and Choi, K. Y. (2000) *Biochemistry 39*, 4581−4589.
41. Edwards, R. A., Whittaker, M. M., Whittaker, J. W., Baker, E. N., and Jameson, G. B. (2001) *Biochemistry 40*, 15−27.
42. Zhang, Z.-Y., Malachowski, W. P., Van Etten, R. L., and Dixon, J. E. (1994) *J. Biol. Chem. 269*, 8140−8145.
43. Dillet, V., Van Etten, R. L., and Bashford, D. (2000) *J. Phys. Chem. B 104*, 11321−11333.
44. Denu, J. M., Zhou, G., Guo, Y., and Dixon, J. E. (1995) *Biochemistry 34*, 3396−3403.
45. Czyryca, P. G., and Hengge, A. C. (2001) *Biochim. Biophys. Acta 1547*, 245−253.
46. Kim, J.-H., Shin, D. Y., Han, M.-H., and Choi, M.-U. (2001) *J. Biol. Chem. 276*, 27568−27574.
47. Zhang, Z.-Y. (1995) *J. Biol. Chem. 270*, 11199−11204.
48. Taga, E. M., and Van Etten, R. L. (1982) *Arch. Biochem. Biophys. 214*, 505−515.
49. Lawrence, G. L., and Van Etten, R. L. (1981) *Arch. Biochem. Biophys. 206*, 122−131.
50. Sklenar, V., Brooks, B. R., Zon, G., and Bax, A. (1987) *FEBS Lett. 216*, 249−252.
51. Sklenar, V., and Bax, A. (1987) *J. Magn. Reson. 74*, 469−479.
52. Markley, J. L. (1973) *Biochemistry 12*, 2245−2250.
53. Zhou, M., and Van Etten, R. L. (1999) *Biochemistry 38*, 2636−2646.
54. Zhang, M., Zhou, M., Van Etten, R. L., and Stauffacher, C. V. (1997) *Biochemistry 36*, 15−23.
55. Wo, Y.-Y., McCormack, A. L., Shabanowitz, J., Hunt, D. F., Davis, J. P., Mitchell, G. L., and Van Etten, R. L. (1992) *J. Biol. Chem. 267*, 10856−10865.
56. Su, X. D., Taddei, N., Stefani, M., Ramponi, G., and Nordlund, P. (1994) *Nature 370*, 575−578.

BI0203740